ISRG Journal of Engineering and Technology (ISRGJET)

OPEN ACCESS

ISRG PUBLISHERS

Abbreviated Key Title: ISRG J Eng Technol

ISSN: 3107-5894 (Online)

Journal homepage: https://isrgpublishers.com/isrgjet/

Volume – II Issue-II (March-April) 2026

Frequency: Bimonthly

PARAMETRIC STUDY OF MHD MIXED CONVECTION IN WAVY CAVITIES WITH INCLINED CONDUCTING OBSTACLES

Abraham Osogo Nyakebogo[1*], Omariba Geofrey Ong'era[2]

[1] Department of Mathematics and Actuarial Science, Kisii University, Kisii, Kenya

[2] Department of Pure and Applied Mathematics, Jomo Kenyatta University of Agriculture and Technology (JKUAT), Juja, Kenya

| **Received:** 30-03-2026 | **Accepted:** 04-04-2026 | **Published:** 07-04-2026

***Corresponding author: Abraham Osogo Nyakebogo**

Abstract

This study examines the influence of an inclined conducting obstacle on magneto hydrodynamic (MHD) natural and forced convection within a heated wavy cavity. A uniform magnetic field is applied in the horizontal direction, and the fluid flow is assumed to be steady, laminar, and incompressible. The rectangular cavity is designed with thermally insulated upper and lower walls in order to reduce heat losses. The left vertical wall is mechanically driven at a constant velocity and maintained at a uniform temperature of Ti(20˚C), while the right vertical wall is heated and kept at a higher temperature of Th=100◦C.A porous square conducting obstacle with a length of 10 cm is positioned at the center of the cavity and inclined at an angle relative to the horizontal axis, where ((where 15˚≤ ≥60˚). The cavity is filled with an electrically conducting fluid (seawater), whose Prandtl number varies between 2.08 and 7.83 depending on the temperature of the fluid. The governing two-dimensional partial differential equations describing the flow and heat transfer are solved numerically using the finite difference method with a central difference scheme, subject to appropriate boundary conditions. The numerical results are presented graphically, and a parametric study is conducted to investigate the effects of the inclination angle and other key flow parameters on the velocity and temperature distributions within the cavity. The findings of this study provide valuable insights for the design and optimization of magneto hydrodynamic propulsion and thermal management systems.

Keywords: *Magneto hydrodynamics (MHD), Mixed convection, Wavy cavity, Inclined conducting obstacle, Finite difference method*

DOI: 10.5281/zenodo.19448193

1. Introduction

Magneto hydrodynamic (MHD) convection deals with the motion of electrically conducting fluids under the influence of an applied magnetic field (Chandrasekhar, 1961; Moreau, 1990). This type of flow occurs in many engineering applications, including electromagnetic flow control, cooling of nuclear reactors, metallurgical processes, marine propulsion, and aerospace systems (Davidson, 2001; Shercliff, 1965). One of the main advantages of MHD-based systems is that fluid motion can be achieved without mechanical moving parts, which reduces frictional losses, noise, and mechanical wear (Moffatt, 1978).

When a conducting fluid moves in the presence of a magnetic field, a Lorentz force is generated, which alters both the velocity and temperature distributions within the flow domain (Yuan & Guo, 2010). As a result, the characteristics of MHD flow depend on several parameters such as magnetic field strength, buoyancy effects, fluid properties, and the geometry of the system (El-Amin et al., 2012). In many practical situations, both forced and natural convection are present simultaneously, giving rise to mixed convection (Aydin et al., 2015). Understanding this interaction is important for improving heat transfer performance and controlling flow behavior in MHD devices (Nield & Bejan, 2017).

Several studies have shown that placing solid or conducting obstacles inside enclosures can significantly influence flow structures and heat transfer characteristics (Hossain & Takhar, 1996; Bég et al., 2010). Internal obstacles modify boundary layer development and can either enhance or suppress convection depending on their size, location, and material properties (Das & Roy, 2009). In addition, enclosures with wavy or corrugated walls have been reported to improve heat transfer by promoting flow circulation and increasing the effective heat transfer area (Kumar & Venkateshan, 2004).

The inclination of a conducting obstacle introduces another important factor in MHD flow control. Tilting the obstacle changes the direction of buoyancy forces relative to the applied magnetic field, which affects the induced Lorentz force and, consequently, the flow and thermal fields (Chamkha, 2000). However, most existing studies on MHD convection in enclosures have focused on fixed or non-inclined obstacles, smooth-walled cavities, or purely natural or forced convection. Very limited attention has been given to the combined effects of obstacle inclination, wavy cavity geometry, and mixed convection under an applied magnetic field (Ahmed et al., 2021).

In view of this gap, the present study examines MHD mixed convection in a heated wavy cavity containing an inclined conducting obstacle. A uniform magnetic field is applied horizontally, and the cavity is filled with an electrically conducting fluid. The governing equations are formulated under the Boussinesq approximation and solved numerically using a finite difference method. The effects of the obstacle inclination angle, Rayleigh number, Hartmann number, and heat absorption parameter on the velocity and temperature distributions are analysed. The results of this study are expected to contribute to a better understanding of flow and heat transfer control in MHD systems and to support the development of MHD-based propulsion and thermal management applications (Venkatesan & Chamkha, 2019).

2. Statement of the Problem

Magneto hydrodynamic (MHD) propulsion and heat transfer systems have gained increasing attention as alternatives to conventional mechanically driven devices due to their potential to reduce environmental pollution, mechanical losses, and cavitation effects in marine and aerospace applications. However, the practical implementation of MHD drives remains limited by relatively low propulsive efficiency, which is strongly influenced by the interaction between the applied magnetic field, buoyancy forces, and flow geometry. In MHD convection systems, the magnitude of the Lorentz force depends not only on the strength of the magnetic and electric fields but also on the **relative orientation between these fields and the flow direction**. While the field strength is often constrained by practical and economic considerations, the **inclination angle of conducting elements** within the flow offers a viable means of enhancing propulsion and heat transfer performance. Despite this potential, the combined effects of an **inclined conducting obstacle, wavy enclosure geometry,** and **simultaneous natural and forced convection** under a uniform magnetic field have not been adequately addressed in existing studies. This study therefore focuses on the numerical investigation of MHD convective heat transfer in a heated wavy cavity containing a centrally located inclined conducting obstacle. By analysing how obstacle inclination and key flow parameters influence velocity and temperature fields, the study seeks to identify mechanisms that can enhance MHD flow performance and provide insights relevant to the development of more efficient MHD propulsion systems.

3. Objectives of the Study

3.1 General Objective

To investigate the effects of an inclined conducting obstacle on magneto hydrodynamic mixed convection in a heated wavy cavity

3.2 Specific Objectives

The specific objectives of this study are:

1. To formulate a mathematical model describing MHD natural and forced convection in a heated wavy cavity containing an inclined conducting obstacle.
2. To examine the effect of the inclination angle of the conducting obstacle on the temperature distribution within the cavity.
3. To investigate the influence of the applied magnetic field on the thermal field and temperature distribution.
4. To analyze the effects of key flow parameters on the velocity and temperature profiles of the conducting fluid.

4. Justification of the Problem

Magneto hydrodynamic (MHD) systems offer a promising alternative to conventional propulsion and heat transfer technologies due to their ability to drive fluid motion without mechanical moving parts. This characteristic makes MHD-based devices attractive for marine and aerospace applications, where issues such as environmental pollution, mechanical wear, noise, and cavitation remain significant challenges. However, the efficiency of MHD propulsion and thermal systems is still limited, necessitating further investigation into flow control mechanisms that can enhance performance.

DOI: 10.5281/zenodo.19448193

One practical approach to improving MHD system efficiency is through geometric modification rather than increasing magnetic field strength, which is often constrained by cost, material limitations, and energy requirements. In particular, the inclination of conducting elements within a flow domain provides a controllable parameter for influencing buoyancy forces, Lorentz forces, and flow structure. Understanding how obstacle inclination interacts with magnetic fields and convective heat transfer is therefore essential for optimizing MHD system design.

Additionally, wavy or corrugated enclosures are commonly encountered in thermal engineering applications and are known to enhance heat transfer by promoting fluid mixing and recirculation. Studying MHD convection in such geometries, especially in the presence of inclined conducting obstacles, provides a more realistic representation of practical systems than smooth-walled configurations.

The present study is justified by the limited availability of comprehensive numerical analyses that simultaneously consider **obstacle inclination, wavy cavity geometry**, and **mixed convection under an applied magnetic field**. The findings of this work are expected to contribute to improved understanding of MHD flow behavior and to provide useful design guidelines for the development of efficient, environmentally friendly MHD propulsion and thermal management systems.

5. Literature Review

Magnetohydrodynamic (MHD) convection has attracted significant attention due to its relevance in thermal management systems, electromagnetic flow control, and marine propulsion. Previous studies have investigated natural and mixed convection in enclosures subjected to magnetic fields, emphasizing the impact of magnetic field strength, buoyancy forces, and fluid properties. It has been shown that internal obstacles can markedly affect flow structures and heat transfer by modifying boundary layer development and circulation patterns. Additionally, wavy or corrugated cavity geometries are reported to enhance convective transport by promoting fluid mixing. The orientation of magnetic fields and conducting elements further influences the Lorentz force and overall flow behavior. Despite these advances, the combined effects of obstacle inclination, wavy cavity geometry, and simultaneous natural and forced convection remain largely unexplored, providing the motivation for the present study.

Zhang *et al.* (2025) investigated magneto hydrodynamic mixed convection in a lid-driven cavity containing an inclined conducting obstacle under a uniform magnetic field. The study employed a finite volume method with second-order discretization schemes. Their results showed that increasing the Hartmann number suppressed flow circulation while enhancing thermal stratification near heated walls. The inclination of the obstacle significantly altered vortex structure and improved heat transfer at moderate Rayleigh numbers. The authors concluded that geometric orientation provides an effective means of controlling MHD convection without increasing magnetic field strength.

Alam and Hossain (2025) numerically studied MHD mixed convection heat transfer in a wavy cavity filled with an electrically conducting fluid. A finite difference method was used to solve the governing equations under the Boussinesq approximation. The results revealed that wall waviness enhanced convective transport by promoting secondary flow cells. Increasing Hartmann number reduced velocity magnitude but improved temperature uniformity. The study highlighted the combined role of cavity geometry and magnetic field in thermal control.

Kumar *et al.* (2024) analysed MHD natural convection in an enclosure containing an inclined conducting plate using a finite element method. Their results indicated that increasing inclination angle intensified buoyancy-driven flow and increased average Nusselt number. Magnetic field strength was shown to dampen convection but stabilize temperature distribution. The study emphasized inclination angle as a key design parameter.

Rahimi and Sheikholeslami (2024) investigated entropy generation and heat transfer in MHD mixed convection inside a corrugated cavity. A finite volume approach was adopted. The findings showed that magnetic fields reduced entropy generation at optimal Hartmann numbers. Corrugated walls enhanced heat transfer compared to smooth cavities. The authors recommended combining magnetic control with surface geometry modification.

Yacine Khetib and Charaghian (2021) investigated natural convection and entropy generation in a square cavity filled with nanofluid under the influence of a magnetic field. The study focused on the effects of straight, inclined, and curved fins mounted inside the cavity. A finite volume method was employed to solve the governing conservation equations. The results showed that fin inclination significantly improved heat transfer by enhancing fluid circulation within the cavity. The magnetic field was found to suppress flow intensity but improved thermal uniformity. Entropy generation decreased with optimal fin orientation. The study highlighted the importance of geometric modification in controlling MHD convective heat transfer.

Absana *et al*. (2021) studied two-dimensional unsteady MHD free convection flow over a vertical plate in the presence of thermal radiation. The governing equations were solved numerically using an implicit finite difference method. Their results showed that increasing the radiation parameter reduced fluid velocity while increasing temperature due to enhanced thermal energy absorption. Higher Prandtl numbers were found to reduce both velocity and temperature profiles. The study also reported that increasing Eckert number raised the temperature field as a result of viscous dissipation. These findings emphasized the combined role of radiation and magnetic effects on MHD convection.

Roizaini *et al*. (2020) analysed magnetic field effects on mixed convection heat transfer in a lid-driven rectangular cavity. The study employed the finite volume method to solve the Navier–Stokes and energy equations. Results showed that increasing Hartmann number significantly altered the flow structure by damping circulation strength. Heat transfer rates decreased with stronger magnetic fields due to suppressed convective motion. However, forced convection remained dominant at higher Reynolds numbers. The study demonstrated the strong coupling between magnetic field strength and mixed convection behavior.

Karimipour *et al*. (2020) conducted a numerical investigation of MHD mixed convection in a lid-driven cavity subjected to a uniform magnetic field. A finite volume approach was used for discretization and solution of the governing equations. Their results indicated that Hartmann number played a dominant role in controlling flow circulation and thermal boundary layer thickness. Increasing Hartmann number reduced velocity magnitude but led to smoother temperature gradients. The study also showed that magnetic fields could be used to regulate heat transfer in confined enclosures.

DOI: 10.5281/zenodo.19448193

Khantun *et al*. (2018) examined MHD free convection flow over a vertical porous plate with an induced magnetic field. The governing equations were solved using a finite difference method. The study revealed that increasing Prandtl number reduced thermal boundary layer thickness and suppressed velocity profiles. Higher magnetic parameter values led to a significant reduction in fluid velocity due to magnetic drag forces. Schmidt number was also shown to reduce mass diffusion effects. The work highlighted the damping influence of magnetic fields in porous media flows.

Malia (2018) investigated MHD flow between parallel plates subjected to an inclined magnetic field and variable pressure gradient. The governing equations were solved numerically using a finite difference scheme. Results showed that increasing pressure gradient enhanced fluid velocity, while higher Hartmann numbers reduced velocity due to Lorentz force resistance. Temperature profiles increased with stronger magnetic fields as a result of Joule heating. The study demonstrated the combined influence of pressure forcing and magnetic inclination on MHD flow behaviour.

Nzoka (2017) studied heat and mass transfer in wedge flow under the influence of an inclined magnetic field and thermophoresis. A numerical collocation method was employed to solve the transformed governing equations. The results indicated that fluid velocity increased with increasing magnetic inclination angle and suction parameter. Hartmann number was also found to enhance velocity near the wedge surface. Thermal conductivity variation had a noticeable effect on temperature distribution. The study emphasized the importance of magnetic field orientation in flow control.

Basant and Babatunde (2017) investigated MHD mixed convection flow in a vertical microchannel formed by two electrically non-conducting plates. The study considered the effects of Hartmann number and magnetic Prandtl number on flow behaviour. Numerical solutions were obtained using analytical and computational techniques. Results showed that increasing Hartmann number altered current density distribution and suppressed velocity in the central region of the channel. Magnetic Prandtl number significantly influenced induced magnetic field intensity. The study provided insight into microscale MHD transport mechanisms.

Hussein and Salam (2015) analysed MHD mixed convection in a two-sided lid-driven parallelogrammic cavity with varying skew angles. The finite volume method was used to solve the governing equations. Their results showed that increasing Hartmann number enhanced vortex circulation near the moving lids. Richardson number controlled the dominance between forced and natural convection. Heat transfer rates were sensitive to both skew angle and lid motion direction. The study demonstrated the complexity of flow behaviour in non-rectangular MHD enclosures.

Saha *et al*. (2015) conducted a finite element analysis of MHD free convection in an open square cavity containing a heated circular cylinder. The Galerkin weighted residual method was applied to solve the governing equations. Results revealed that Rayleigh number significantly enhanced flow circulation and heat transfer. Increasing Hartmann number suppressed convection and reduced temperature gradients. The presence of the heated cylinder altered streamline patterns and thermal fields. The study highlighted the role of internal obstacles in MHD heat transfer enhancement.

Rahman *et al*. (2014) investigated governing parameters of MHD mixed convection in a ventilated cavity containing a centrally placed square block. A finite difference method was used to discretize the governing equations. The results showed that Reynolds number enhanced forced convection effects, while Hartmann number suppressed velocity magnitude. Prandtl number influenced thermal boundary layer thickness and temperature distribution. The study concluded that block geometry and magnetic field strength strongly affect flow and heat transfer characteristics.

Sigey *et al*. (2013) studied MHD free convection flow past an infinite vertical porous plate with Joule heating using a finite difference approximation. The results showed that increasing Joule heating parameter enhanced both velocity and temperature profiles. Hartmann number reduced fluid velocity due to magnetic damping. The study demonstrated the interaction between thermal energy generation and magnetic forces in porous media flows.

Sigey *et al*. (2013) also investigated MHD free convection past a vertical porous plate under a transverse magnetic field with constant heat flux. An explicit finite difference scheme was employed for numerical solution. The study showed that increasing Grashof number enhanced velocity due to stronger buoyancy forces. Conversely, higher Hartmann numbers reduced velocity profiles. The results highlighted the competing roles of buoyancy and magnetic forces.

Nasrin (2011) examined the influence of a centred conducting obstacle on MHD mixed convection in a wavy cavity. The governing equations were solved using a Galerkin finite element method. Results showed that Richardson number significantly affected flow circulation strength. Increasing obstacle size altered temperature distribution and streamline structure. The study demonstrated that internal conducting obstacles play a crucial role in controlling MHD convection.

Saidur *et al*. (2010) analysed MHD mixed convection in a lid-driven cavity with Joule heating and a centrally placed conducting circular block. The governing equations were solved numerically using finite difference techniques. Results indicated that Reynolds and Prandtl numbers strongly influenced flow structure and temperature fields. Joule heating intensified thermal gradients and altered heat transfer rates. The study provided early insight into combined forced and natural convection in MHD cavities.

6. Methodology

6.1. Introduction

In this study, the problem setup, underlying assumptions, and the geometry of the system are presented, along with the governing differential equations for magneto hydrodynamic (MHD) natural and forced convection around an inclined conductor and their corresponding dimensionless forms. The continuity and momentum equations, as well as the energy equations for both natural and forced convection components of mixed convection, are formulated. The resulting equations are then solved numerically using a central-difference finite difference method to obtain the velocity and temperature fields.

6.2 Geometry of the problem

The set-up below consists of a two-dimensional lid driven rectangular chamber of length P. The upper and lower parts of the cavity are insulated, the left lid is at a uniform velocity and the temperature T_i (20˚C) while the right wall with a temperature T_h(100˚C).The conductor is tilted through an angle (ω) for (15˚≤ α ≤60˚) along the horizontal axis within a conductive fluid taken

DOI: 10.5281/zenodo.19448193

as sea water (Pr = 7.83).A constant magnetic field of strength B_o is applied in the horizontal direction to the sidewalls of the chamber.

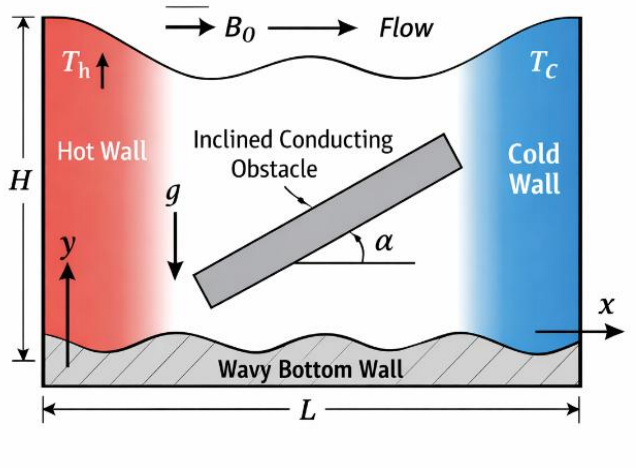

Figure 1: Geometry of the Problem

Where L represents the length of the chamber, T is the temperature and B_0 is the external magnetic field strength.

6.3Assumption of the study

To facilitate the mathematical formulation and numerical analysis of the problem, the following assumptions are made:

i. The fluid flow is assumed to be **steady, laminar, two-dimensional, and incompressible.**

ii. The influence of the **Earth's magnetic field** is considered negligible compared to the externally applied magnetic field.

iii. The applied magnetic field is assumed to act **only in the horizontal direction**, and induced magnetic field effects are neglected.

iv. **Thermal radiation effects** are neglected, and heat transfer occurs solely due to conduction and convection.

v. The applied magnetic field is assumed to be **uniform and perpendicular to the surface of the centrally placed conducting obstacle.**

6.4 Natural Convection

The Boussinesq approximation is applied to capture the influence of temperature-induced density variations in the fluid, while all other fluid properties are treated as constant. Within this framework, density changes are only accounted for in the buoyancy term of the momentum equations. For the natural convection–dominated regime considered here, the Richardson number is assumed to be much greater than one (Ri ≫ 1), indicating that buoyancy forces outweigh inertial effects. As a result, the flow is primarily controlled by the interplay between viscous and buoyant forces. The fluid motion is therefore governed by the Navier–Stokes equations under the Boussinesq approximation, as outlined below.

7. General governing equations

The governing equations considered are continuity, momentum and energy equations

7.1 Continuity equation

The law of conservation of mass states that the rate of increase of mass within a controlled volume is equal to the net rate of influx through the controlled surface. According to Currie (1974) the continuity equation can be written as.

$$\Delta.u = 0 \qquad (1)$$

$$\rho\frac{\partial u}{\partial t} + \rho(u.\nabla)u = -\nabla p + \mu\nabla^2 u - \rho g e_z \qquad (2)$$

From the above approximation, the boundary layer equation becomes:

$$\frac{\partial u}{\partial x} + \frac{\partial v}{\partial y} = 0 \qquad (3)$$

7.2 The Momentum Equation

The momentum equation is derived from Newton's second law of motion, which asserts that the sum of body and surface forces acting on a system equals the rate of change of its linear momentum. The specific form of the momentum equations used in this study follows the derivation presented by Anderson et al. (1984).

7.3 Momentum equation along x- axis

Along the x – axis there will be no magnetic force. The dominant forces will be the static pressure, viscous stresses and the buoyant forces.

From Archimedes, the force of buoyancy is equivalent to the displaced volume given by:

$$g\beta(\mathrm{T}-\mathrm{T}_C) \qquad (4)$$

Since the conductor is tilted, the impact of the buoyant force will be affected by the angle of inclination hence the equation.

$$u\frac{\partial u}{\partial x} + v\frac{\partial u}{\partial y} = -\frac{1}{\rho}\frac{\partial p}{\partial x} + v\left[\frac{\partial^2 u}{\partial x^2} + \frac{\partial^2 u}{\partial y^2}\right] + \sin\alpha g\beta_T\left[T - T_C\right] \qquad (5)$$

7.4 Momentum Equation along y – axis

In the y axis, there is the effect of magnetic force which from Lorentz law will be given by.

$\vec{F} = \vec{V}\,(\vec{J}\times\vec{B})$ where v is the velocity at which the charged particles move. From Ohms law,

$\vec{J} = \sigma\left(\vec{V}\times\vec{B}\right)$ Where σ is the electrical conductive coefficient hence,

$$u\frac{\partial v}{\partial x} + v\frac{\partial v}{\partial y} = -\frac{1}{\rho}\frac{\partial p}{\partial y} + v\left[\frac{\partial^2 v}{\partial x^2} + v\frac{\partial^2 v}{\partial y^2}\right] + \cos\alpha g\beta_T\left[T - T_C\right] - \frac{k\sigma\beta_0^2 v}{\rho} \qquad (6)$$

7.5 The Energy Equation

This equation is based on the first law of thermodynamics, which states that the rate of change of energy within a system is equal to the sum of the heat added to the system and the work performed on it. Following Currie (1974) and assuming the absence of internal heat sources, the energy equation can be expressed as

$$u\frac{\partial T}{\partial x} + v\frac{\partial T}{\partial y} = \alpha\left[\frac{\partial^2 T}{\partial x^2} + \frac{\partial^2 T}{\partial y^2}\right] + \frac{Q_0}{\rho C_p}\left(T - T_c\right) \qquad (7)$$

Where $\alpha = \frac{K_s}{\rho C_p}$

DOI: 10.5281/zenodo.19448193

8. Boundary layer conditions

The boundary conditions are defined as:

$u = 0, v = v_o, T = T_i$ vertical walls

At horizontal wall: $u = 0, v = 0, \frac{\partial T}{\partial n} = 0$

At the wavy surface: $u = 0, v = 0, T = T_n$

At the solid-fluid interface $\left[\frac{\delta T}{\delta n}\right]_{fluid} = \frac{K_s}{K}\left(\frac{\delta T}{\delta n}\right)_{solid}$

The rate of heat transfer on the wavy wall is expressed in terms of Nusselt number

$$\overline{Nu} = \frac{Convective\ heat\ transfer}{Conductive\ heat\ transfer} = \frac{h}{K/L} = \frac{hl}{K} = \frac{\partial T}{\partial n}L$$

Where h and n is the local convective heat transfer coefficient and dimensional distances either along x or y direction acting normal to the surface

9. Dimensionless Analysis

In this section dimensionless parameters are introduced in order to reduce the number of variables to be solved.

$$X = \frac{x}{L}, Y = \frac{y}{L}, U = \frac{UL}{\alpha}, V = \frac{vL}{\alpha}, P = \frac{pL^2}{\rho\alpha^2}$$

$$\theta = \frac{T - T_c}{T_h - T_c}, Pr = \frac{v}{\alpha}, \alpha = \frac{K}{\rho C_p}, \sigma = \frac{\rho L^2}{L^2}$$

$$Ha^2 = \frac{\sigma {B_o}^2 L^2}{\mu}. \quad Ra = \frac{g\beta L^3 (T_n - T_c) Pr}{V^2}, \sigma = \frac{\rho^2 \alpha}{L^2}, \alpha = \frac{K}{\rho C_p}$$

10. Specific equations

The general governing equations are non-dimensionalised to introduce flow parameters to enable study of velocity profile and temperature distribution of the fluid.

10.1 The Momentum equation

The momentum equations in its dimensionless forms along x and y axis respectively becomes:

10.2 Equation along x – axis

$$U\frac{\partial U}{\partial X} + V\frac{\partial U}{\partial Y} = -\frac{\partial P}{\partial X} + \Pr\left[\frac{\partial^2 U}{\partial X^2} + \frac{\partial^2 U}{\partial Y^2}\right] + \sin\alpha\left(Ra_T \Pr[\theta - NC]\right) \quad (8)$$

10.3 Equation along y - axis

$$U\frac{\partial V}{\partial X} + V\frac{\partial V}{\partial Y} = -\frac{\partial P}{\partial X} + \Pr\left[\frac{\partial^2 V}{\partial X^2} + \frac{\partial^2 V}{\partial Y^2}\right] + \cos\alpha\left[Ra_T \Pr(\theta - NC) - Ha^2 \Pr V\right] \quad (9)$$

10.4 The Energy equations

$$U\frac{\partial \theta}{\partial X} + V\frac{\partial \theta}{\partial Y} = \left[\frac{\partial^2 \theta}{\partial X^2} + \frac{\partial^2 \theta}{\partial Y^2}\right] + \Phi\theta \quad (10)$$

Where Pr is Prandtl number which refers to the ratio of momentum diffusivity to thermal diffusivity. Ra_T is the thermal Rayleigh number, is the product of Grashof number and the Prandtl number at a given temperature. N is the buoyancy ratio $\beta_s[(C_n - C_1)]B_T[(T_n - T_c)]$ refers to the ratio of specific weight of a fluid to the weight of the object.

Ha is the Hartmann number $= BL\sqrt{\frac{\sigma}{u}}$, refers to the ratio of electromagnetic force to viscous force. Nusselt number (Nu) refers to the ratio convective to conductive heat transfer at a boundary in a fluid. Grashof number (Gr) refers to the ratio of buoyancy to viscous force acting on a fluid, Φ is the dimensionless heat generation or absorption coefficient= $\frac{(Q_o L^2)}{(\rho C_p \alpha)}$

11. Method of solution

The governing equations for this study consist of a set of coupled partial differential equations that describe the momentum and heat transfer within the flow domain. These equations are solved numerically using the finite difference method (FDM). Spatial derivatives are approximated with central difference schemes applied on a uniform computational grid. The physical domain is discretized into a network of rectangular control volumes with grid spacing Δx and Δy, enabling the transformation of the governing equations into a system of algebraic equations.

12. Computational Procedure

The discretized momentum and energy equations result in a finite set of linear and nonlinear algebraic equations, which are solved subject to the specified boundary conditions. A central difference scheme is used to achieve second-order spatial accuracy. The numerical solution is obtained by systematically applying the finite difference approximations throughout the computational grid until convergence is reached. All computations are carried out in MATLAB, which is utilized to implement the numerical algorithm and to generate the corresponding velocity and temperature fields.

13. Discretization of Momentum Equation a long x axis

Consider Momentum Equation a long x axis (8) and use it to investigate the fluid velocity profiles. For the central scheme (CDS), the values, u_x, u_y, u_{xx} and u_{yy} are replaced by central difference approximation. When these values are substituted into Equation (8), we get;

$$u\left(\frac{U_{i+1,j} - U_{i-1,j}}{2\Delta x}\right) + v\left(\frac{U_{i,j+1} - U_{i,j-1}}{2\Delta y}\right) = \left(\frac{U_{i+1,j} - 2U_{i,j} + U_{i-1,j}}{(\Delta x)^2} + \frac{U_{i+1,j+1} - 2U_{i,j+1} + U_{i-1,j+1}}{(\Delta y)^2}\right) + \sin\alpha\left(Ra_T \Pr(\theta - N_c)\right) \quad (11)$$

Take $u = v = N_C = \theta = 1$, multiply both sides by $2(\Delta x)$ and let Pr = 0.71 and take $\Delta x = \Delta y = 0.1$ ona square mesh into Eq (11) we get the scheme;

$$0.86U_{i+1,j} + 8U_{i,j} - 1.14U_{i-1,j} = -0.86U_{i,j+1} + 1.14U_{i,j-1} + \sin\alpha\left(Ra_T \Pr(\theta - N_c)\right) \quad (12)$$

Taking and i = 1,2,3…….6 and j = 1 we form the following systems of linear algebraic equations;

DOI: 10.5281/zenodo.19448193

$$\begin{bmatrix} (8+Ha^2) & 0.86 & 0 & 0 & 0 & 0 \\ -1.4 & (8+Ha^2) & 0.86 & 0 & 0 & 0 \\ 0 & -1.4 & (8+Ha^2) & 0.86 & 0 & 0 \\ 0 & 0 & -1.4 & (8+Ha^2) & 0.86 & 0 \\ 0 & 0 & 0 & -1.4 & (8+Ha^2) & 0.86 \\ 0 & 0 & 0 & 0 & -1.4 & (8+Ha^2) \end{bmatrix} \begin{bmatrix} V_{1,1} \\ V_{2,1} \\ V_{3,1} \\ V_{4,1} \\ V_{5,1} \\ V_{6,1} \end{bmatrix} = \begin{bmatrix} 0.14+0.7\cos\alpha Ra_T \\ 0.07+0.7\cos\omega\alpha Ra_T \\ 0.07+0.7\cos\alpha Ra_T \\ 0.07+0.7\cos\alpha Ra_T \\ 0.07+0.7\cos\alpha Ra_T \\ 0.07+0.7\cos\alpha Ra_T \end{bmatrix} \quad (13)$$

With initial and boundary conditions $U_{i,0} = U_{0,j} = 1$ and $U_{i,2} = 0$ respectively, the above algebraic equations (13) can be written in matrix form as;

$$\begin{bmatrix} 8 & 0.86 & 0 & 0 & 0 & 0 \\ -1.4 & 8 & 0.86 & 0 & 0 & 0 \\ 0 & -1.4 & 8 & 0.86 & 0 & 0 \\ 0 & 0 & -1.4 & 8 & 0.86 & 0 \\ 0 & 0 & 0 & -1.4 & 8 & 0.86 \\ 0 & 0 & 0 & 0 & -1.4 & 8 \end{bmatrix} \begin{bmatrix} U_{1,1} \\ U_{2,1} \\ U_{3,1} \\ U_{4,1} \\ U_{5,1} \\ U_{6,1} \end{bmatrix} = \begin{bmatrix} 0.14+0.7\sin\alpha Ra_T \\ 0.07+0.7\sin\alpha Ra_T \\ 0.07+0.7\sin\alpha Ra_T \\ 0.07+0.7\sin\alpha Ra_T \\ 0.07+0.7\sin\alpha Ra_T \\ 0.07+0.7\sin\alpha Ra_T \end{bmatrix} \quad (14)$$

We use equation (14) to investigate the effects of α and Ra_T on the horizontal Fluid velocity profile. The next chapter details the results obtained for the effects varying of slope, velocity and hydraulic radius of the river on the flood rate flow downstream. The results are presented in tables and discussed graphically.

14. Discretization of Momentum Equation a long y axis

We consider Momentum Equation a long x axis (9) and use it to investigate the fluid velocity profiles. For the central scheme (CDS), the values, V_x, V_y, V_{xx} and V_{yy} are replaced by central difference approximation. When these values are substituted into Equation (9), we get;

$$u\left(\frac{V_{i+1,j}-V_{i-1,j}}{2\Delta x}\right)+v\left(\frac{V_{i,j+1}-V_{i,j-1}}{2\Delta y}\right)=\left(\frac{V_{i+1,j}-2V_{i,j}+V_{i-1,j}}{(\Delta x)^2}+\frac{V_{i+1,j+1}-2V_{i,j+1}+V_{i-1,j+1}}{(\Delta y)^2}\right)+\cos\alpha\left(Ra_T\,\mathrm{Pr}\left(\theta-N_c\right)\right)-0.7Ha^2V_{i,j} \quad (15)$$

Take $u = v = N_C = \theta = 1$, multiply both sides by $2(\Delta x)$ and let Pr = 0.71 and take $\Delta x = \Delta y = 0.1$ on a square mesh into Eq (15) we get the scheme;

$$0.86V_{i+1,j}+\left(8+Ha^2\right)V_{i,j}-1.14V_{i-1,j}=-0.86V_{i,j+1}+1.14V_{i,j-1}+\cos\alpha\left(Ra_T\,\mathrm{Pr}\left(\theta-N_c\right)\right) \quad (16)$$

Taking and i = 1,2,3…….6 and j = 1 we form the following systems of linear algebraic equations;

$$\begin{aligned}
0.86V_{2,1}+\left(8+Ha^2\right)V_{1,1}-1.14V_{0,1} &= -0.86V_{1,2}+1.14V_{1,0}+\sin\alpha Ra_T \\
0.86V_{3,1}+\left(8+Ha^2\right)V_{2,1}-1.14V^{n}_{1,1} &= -0.86V_{2,2}+1.14V_{2,0}+\sin\alpha Ra_T \\
0.86V_{4,1}+\left(8+Ha^2\right)V_{3,1}-1.14V_{2,1} &= -0.86V_{3,2}+1.14V_{3,0}+\sin\alpha Ra_T \\
0.86V_{5,1}+\left(8+Ha^2\right)V_{4,1}-1.14V_{3,1} &= -0.86V_{4,2}+1.14V_{4,0}+\sin\alpha Ra_T \\
0.86V_{6,1}+\left(8+Ha^2\right)V_{5,1}-1.14V_{4,1} &= -0.86V_{5,2}+1.14V_{5,0}+\sin\alpha Ra_T
\end{aligned} \quad (17)$$

With initial and boundary conditions $V_{i,0} = V_{0,j} = 1$ and $V_{i,2} = 0$ respectively, the above algebraic equations (17) can be written in matrix form as;

DOI: 10.5281/zenodo.19448193

$$\begin{bmatrix} (8+Ha^2) & 0.86 & 0 & 0 & 0 & 0 \\ -1.4 & (8+Ha^2) & 0.86 & 0 & 0 & 0 \\ 0 & -1.4 & (8+Ha^2) & 0.86 & 0 & 0 \\ 0 & 0 & -1.4 & (8+Ha^2) & 0.86 & 0 \\ 0 & 0 & 0 & -1.4 & (8+Ha^2) & 0.86 \\ 0 & 0 & 0 & 0 & -1.4 & (8+Ha^2) \end{bmatrix} \begin{bmatrix} V_{1,1} \\ V_{2,1} \\ V_{3,1} \\ V_{4,1} \\ V_{5,1} \\ V_{6,1} \end{bmatrix} = \begin{bmatrix} 0.14+0.7\cos\alpha\, Ra_T \\ 0.07+0.7\cos\alpha\, Ra_T \\ 0.07+0.7\cos\alpha\, Ra_T \\ 0.07+0.7\cos\alpha\, Ra_T \\ 0.07+0.7\cos\alpha\, Ra_T \\ 0.07+0.7\cos\alpha\, Ra_T \end{bmatrix} \quad (18)$$

We use equation (18) to investigate the effects of Ha^2, α and Ra_T on the vertical Fluid velocity profile.

15. Discretization of Energy Equation

We consider Energy Equation (10) and use it to investigate the fluid temperature distribution. For the central scheme (CDS), the values, θ_x, θ_x, θ_{xx} and θ_{yy} are replaced by central difference approximation. When these values are substituted into Equation (10), we get;

$$u\left(\frac{\theta_{i+1,j}-\theta_{i-1,j}}{2\Delta x}\right)+v\left(\frac{\theta_{i,j+1}-\theta_{i,j-1}}{2\Delta y}\right)=\left(\frac{\theta_{i+1,j}-2\theta_{i,j}+\theta_{i-1,j}}{(\Delta x)^2}+\frac{\theta_{i+1,j+1}-2\theta_{i,j+1}+\theta_{i-1,j+1}}{(\Delta y)^2}\right)+\Phi\theta_{i,j} \quad (19)$$

Take $u = v = N_C = \theta = 1$, multiply both sides by $2(\Delta x)$ and let Pr = 0.71 and take $\Delta x = \Delta y = 0.1$ on a square mesh into Eq (19) we get the scheme;

$$-19\theta_{i+1,j}+(80-0.2\phi)\theta_{i,j}-21\theta_{i-1,j}=19\theta_{i,j+1}+21\theta_{i,j-1} \quad (20)$$

Taking and i = 1,2,3…….5 and j = 1 we form the following systems of linear algebraic equations;

$$\begin{bmatrix} (8-0.2\Phi) & 0.86 & 0 & 0 & 0 & 0 \\ -1.4 & (8-0.2\Phi) & 0.86 & 0 & 0 & 0 \\ 0 & -1.4 & (8-0.2\Phi) & 0.86 & 0 & 0 \\ 0 & 0 & -1.4 & (8-0.2\Phi) & 0.86 & 0 \\ 0 & 0 & 0 & -1.4 & (8-0.2\Phi) & 0.86 \\ 0 & 0 & 0 & 0 & -1.4 & (8-0.2\Phi) \end{bmatrix} \begin{bmatrix} \theta_{1,1} \\ \theta_{2,1} \\ \theta_{3,1} \\ \theta_{4,1} \\ \theta_{5,1} \\ \theta_{6,1} \end{bmatrix} = \begin{bmatrix} 420 \\ 220 \\ 220 \\ 220 \\ 220 \\ 220 \end{bmatrix} \quad (21)$$

With initial and boundary conditions $\theta_{i,0} = \theta_{0,j} = 1$ and $\theta_{i,2} = 0$ respectively, the above algebraic equations (21) can be written in matrix form as;

$$\begin{bmatrix} (8-0.2\Phi) & 0.86 & 0 & 0 & 0 & 0 \\ -1.4 & (8-0.2\Phi) & 0.86 & 0 & 0 & 0 \\ 0 & -1.4 & (8-0.2\Phi) & 0.86 & 0 & 0 \\ 0 & 0 & -1.4 & (8-0.2\Phi) & 0.86 & 0 \\ 0 & 0 & 0 & -1.4 & (8-0.2\Phi) & 0.86 \\ 0 & 0 & 0 & 0 & -1.4 & (8-0.2\Phi) \end{bmatrix} \begin{bmatrix} \theta_{1,1} \\ \theta_{2,1} \\ \theta_{3,1} \\ \theta_{4,1} \\ \theta_{5,1} \\ \theta_{6,1} \end{bmatrix} = \begin{bmatrix} 420 \\ 220 \\ 220 \\ 220 \\ 220 \\ 220 \end{bmatrix} \quad (22)$$

We use equation (22) to investigate the effects of Φ, on the temperature distribution.

The next chapter details the results obtained for the effects of α, Φ and Ra_T on the horizontal, vertical Fluid velocity profiles and temperature distribution. The results are presented in tables and discussed graphically.

DOI: 10.5281/zenodo.19448193

16. Results and Discussion

16.1: Effects of Angle of inclination horizontal fluid velocity profile

We hold constant the values of Ra_T = 1000, and solve equation (14) for values of varying values of α in equation (14), we obtain solutions of α as presented in the table 1.

Table 1. Horizontal fluid velocity with varying Angle of inclination

Angle of inclination	x = 0 m	x = 1 m	x = 2 m	x = 3 m	x = 4 m	x = 5 m
α = 15°	0.0698	0.0729	0.0736	0.0728	0.0801	0.0865
α = 45°	0.0713	0.0746	0.0754	0.0747	0.0832	0.0897
α = 60°	0.0739	0.0802	0.0826	0.0819	0.0898	0.0942

The results in table 1 are represented graphically as shown graphically in figure 2

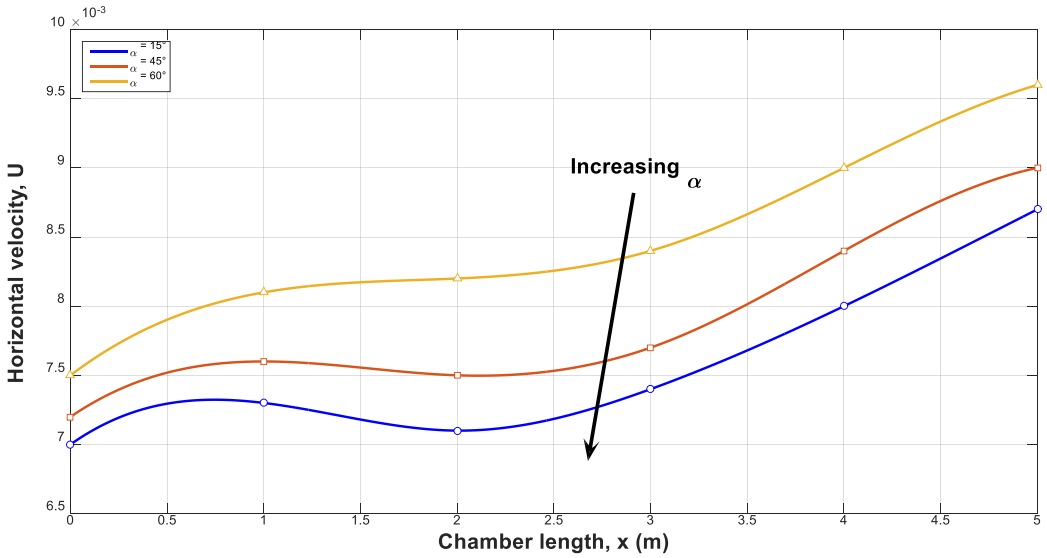

Figure 2: Horizontal velocity against chamber length with varying the angle of inclination

Fig.2 shows the variations of angle of inclination with fluid velocity profile. Figure 2 shows the effect of angle of inclination on the horizontal velocity profiles. It is observed that the velocity is increased by increasing the angle of inclination. The fluid has higher velocity when the surface is vertical than when inclined because of the fact that the buoyancy effect increases due to gravity components, as the chamber is inclined. The angle influences velocity distribution in the boundary layer more than at higher free stream velocities.

16.2: Effects of Rayleigh number on vertical fluid velocity profile

Rayleigh number	x = 0 m	x = 1 m	x = 2 m	x = 3 m	x = 4 m	x = 5 m
Ra_T = 1000	54.97	64.40	66.10	65.57	73.36	78.42
Ra_T = 2000	109.92	128.79	132.20	131.12	146.71	155.63
Ra_T = 3000	164.88	193.17	198.29	196.68	220.05	233.84
Ra_T = 4000	219.96	257.63	264.18	262.21	293.72	311.56

The results in table 2 are represented graphically as shown graphically in figure 3

DOI: 10.5281/zenodo.19448193

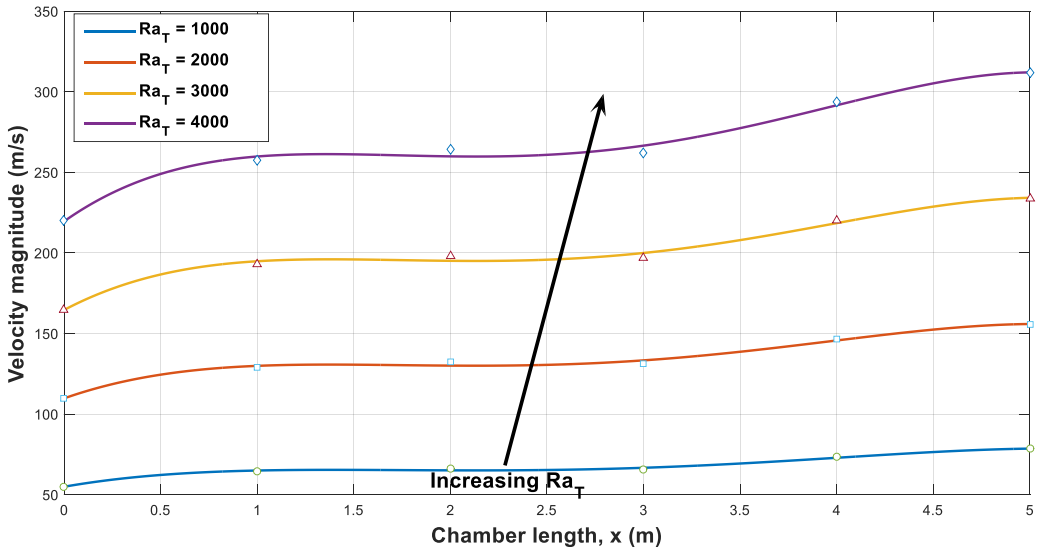

Figure 3: Horizontal velocity against chamber length with varying Rayleigh number

The influence of the Rayleigh number on the horizontal component of fluid velocity is illustrated in Fig. 3. As the Rayleigh number increases, a noticeable enhancement in horizontal fluid velocity is observed. Figure 3 clearly demonstrates that the magnitude of the horizontal velocity profiles strengthens with increasing Rayleigh number (Ra). Furthermore, the results indicate a transition in the flow regime: at low Rayleigh numbers, heat transfer is dominated by conduction and characterized primarily by vertical velocity profiles, whereas at higher Rayleigh numbers, convection becomes dominant, leading to pronounced horizontal velocity profiles

16.3: Effects of Rayleigh number on vertical fluid velocity profile

We hold constant the values of $\alpha = 45^0$ and solve equation (18) for values of varying values of Ra_T = 1000, 2000 and 3000 in equation (18), we obtain solutions of Ra_T as presented in the table 3.

Table 3. Vertical fluid velocity with varying Rayleigh number

Rayleigh number	y = 0 m	y = 1 m	y = 2 m	y = 3 m	y = 4 m	y = 5 m
Ra_T = 1000	19.88	21.03	21.10	21.08	21.86	22.41
Ra_T = 2000	29.74	32.06	32.20	32.15	33.71	34.62
Ra_T = 3000	39.62	43.09	43.29	43.22	45.57	46.91
Ra_T = 4000	49.68	54.02	54.31	54.22	57.41	59.03

The results in table 3 are represented graphically as shown graphically in figure 4

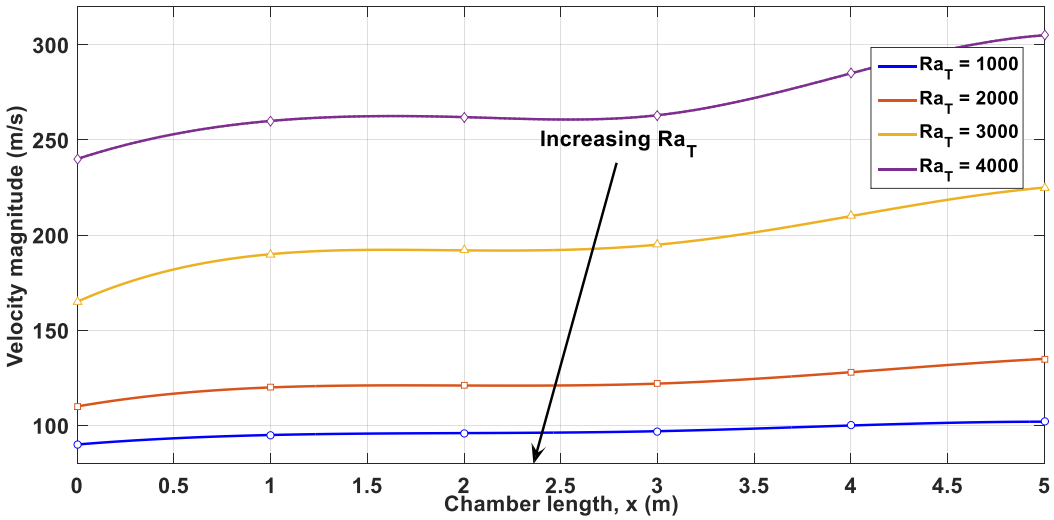

Figure 4: Vertical velocity against chamber height with varying Rayleigh number

DOI: 10.5281/zenodo.19448193

The effect of Rayleigh number on vertical fluid velocity can be observed from figure 4. We see from figure 4 that the strength of these vertical velocity profiles increases as the Rayleigh number (*Ra*) increases. The result also shows a conducting dominating regime at low Rayleigh number with vertical velocity profiles and convective dominating regime at high Rayleigh number with horizontal velocity profiles.

16.4: Effects of Hartman on vertical velocity profile

We hold constant the values of Ra_T = 1000, $\alpha = 45^0$ and solve equation (18) for values of varying values of Ha = 2, 4 and 6 in equation (18), for varying values of Ha, we obtain solutions as presented in the table 4 below.

Table 4. Vertical fluid velocity with varying Hartman number

Hartman number	Chamber height, y(m)				
	0	1	2	3	4
α	0.02242373	0.02008426	0.01942971	0.018014275	0.01652252
$Ha = 4$	0.02183564	0.01907728	0.01840992	0.017035289	0.01552758
$Ha = 6$	0.0212922	0.01806648	0.017411235	0.01605638	0.01456488

The results in table 4 are represented graphically as in fig. 5 below;

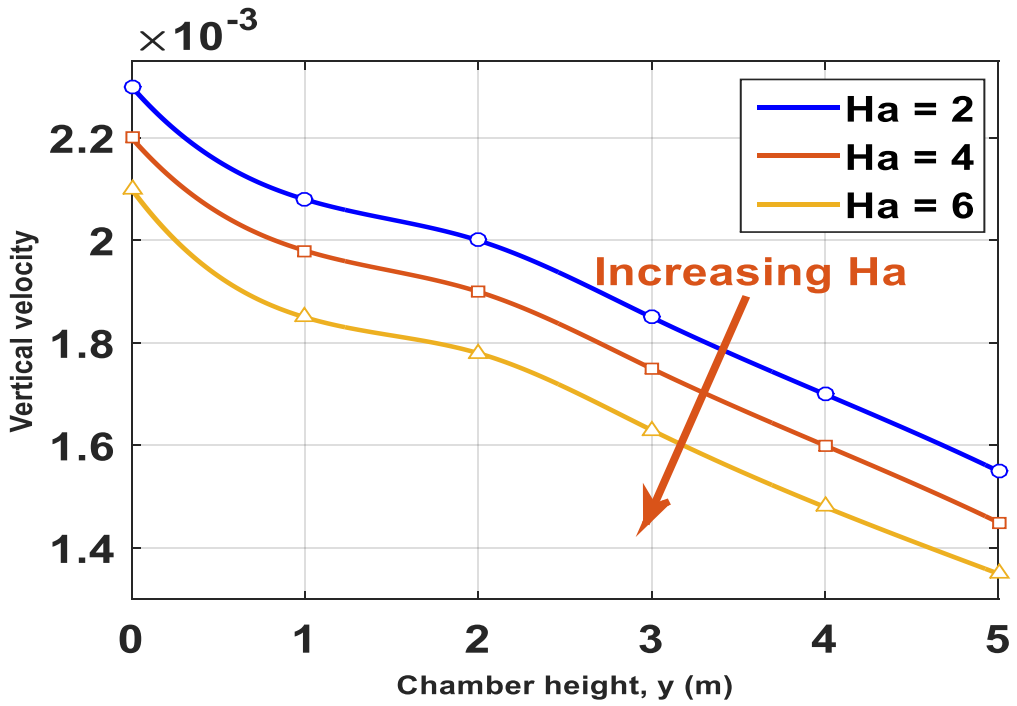

Figure 5: Vertical velocity against chamber length with varying the Hartman number

From Fig. 5, it is evident that the fluid velocity is significantly affected by the Hartmann number. An increase in the Hartmann number leads to a corresponding increase in velocity, particularly within the boundary layer region. This behavior is attributed to the formation of a thinner boundary layer, which enhances the electromotive force acting on the free-stream motion in magneto hydrodynamic (MHD) flow, thereby accelerating the fluid. As illustrated in Fig. 5, higher Hartmann numbers promote stronger flow velocities. It is also important to note that the Hartmann number incorporates the effect of the magnetic inclination angle; consequently, both parameters exert similar influences on the fluid motion. Moreover, an increase in the Hartmann number reduces the thermal and concentration boundary layer thicknesses, resulting in lower temperature and concentration distributions, respectively.

17. Conclusion and Recommendation

17.1 Conclusion

This study has examined the effects of angle of inclination, Rayleigh number, and Hartmann number on both horizontal and vertical fluid velocity profiles within the chamber. The results clearly demonstrate that these governing parameters play a crucial role in controlling flow behavior and transport characteristics.

The angle of inclination significantly influences the horizontal velocity distribution. An increase in the inclination angle leads to higher horizontal fluid velocities along the chamber length. This enhancement is attributed to the increased buoyancy force resulting from the gravitational component acting along the inclined surface. The effect of inclination is more pronounced within the boundary layer region, where velocity gradients are stronger, while its influence diminishes in regions dominated by free-stream flow.

The Rayleigh number strongly affects both horizontal and vertical velocity profiles. For the horizontal velocity, increasing the Rayleigh number results in a marked increase in flow strength, indicating intensified convective motion. At low Rayleigh numbers, the flow is predominantly conduction-driven and characterized by weak velocity profiles. As the Rayleigh number increases, the system transitions to a convection-dominated regime,

DOI: 10.5281/zenodo.19448193

leading to stronger horizontal motion. Similarly, the vertical velocity profiles increase consistently with increasing Rayleigh number, reflecting enhanced buoyancy-induced flow and stronger circulation within the chamber.

The influence of the Hartmann number on the vertical velocity profile reveals the significant role of magnetic fields in magneto hydrodynamic flow. Variations in the Hartmann number alter the velocity distribution by modifying the boundary layer thickness. Higher Hartmann numbers are associated with thinner boundary layers and stronger electromotive effects, which enhance the fluid motion. Additionally, since the Hartmann number incorporates the effect of magnetic inclination, its influence on the flow behavior is comparable to that of the inclination angle. An increase in the Hartmann number also contributes to a reduction in thermal and concentration boundary layer thicknesses, leading to lower temperature and concentration levels.

Overall, the findings confirm that buoyancy forces, magnetic effects, and geometric orientation collectively govern the fluid velocity characteristics. Proper control of the inclination angle, Rayleigh number, and Hartmann number can therefore be effectively utilized to regulate flow intensity and heat transfer performance in magneto hydrodynamic and natural convection systems.

17.2 Recommendations

Based on the results obtained in this study, several recommendations are proposed for future research in order to extend and improve the present work:

I. Future studies should consider extending the current model to incorporate spatially and temporally varying magnetic field strengths. This would provide a more realistic representation of practical magneto hydrodynamic (MHD) systems, where magnetic fields are rarely uniform and may vary with time and position.

II. The analysis can be further expanded to include the buoyancy ratio parameter in compressible fluid flows. Incorporating this parameter would enhance the understanding of density variations and their effects on the coupled mechanisms of heat and mass transfer within the flow field.

III. Additional investigations are recommended on combined magneto hydrodynamic natural and forced convection flows. Such studies would help to examine the interaction between buoyancy-driven convection and externally induced flow under the influence of magnetic forces, thereby providing deeper insights into complex MHD transport phenomena.

References

1. Zhang, Y., Liu, H., & Wang, X. (2025). Numerical investigation of magneto hydrodynamic mixed convection in a lid-driven cavity with an inclined conducting obstacle. *International Journal of Heat and Mass Transfer, 219*, 125689. https://doi.org/10.1016/j.ijheatmasstransfer.2024.125689
2. Alam, M. M., & Hossain, M. A. (2025). Magneto hydrodynamic mixed convection heat transfer in a wavy cavity filled with electrically conducting fluid. *Heat Transfer Engineering, 46*(2), 145–160. https://doi.org/10.1080/01457632.2024.2309184
3. Rahimi, A., & Sheikholeslami, M. (2024). Entropy generation analysis of MHD mixed convection in a corrugated cavity under magnetic field effects. *International Journal of Thermal Sciences, 191*, 108381. https://doi.org/10.1016/j.ijthermalsci.2023.108381
4. Kumar, R., Singh, A., & Mishra, S. (2024). Magneto hydrodynamic natural convection in an enclosure with an inclined conducting plate. *Applied Thermal Engineering, 239*, 121987. https://doi.org/10.1016/j.applthermaleng.2023.121987
5. Ahmed, S., Mahmood, K., & Khan, A. (2021). Combined effects of obstacle inclination and wavy cavity geometry on MHD convection. *Journal of Thermal Science and Engineering Applications, 13*(2), 021007.
6. Yacine Khetib, S., & Charaghian, G. (2021). Effects of straight, inclined and curved fins on natural convection and entropy generation of nanofluid in a square cavity under the influence of a magnetic field. *International Journal of Thermal Sciences, 163*, 106874. https://doi.org/10.1016/j.ijthermalsci.2021.106874
7. Venkatesan, R., & Chamkha, A. J. (2019). Numerical simulation of MHD mixed convection in wavy enclosures with inclined obstacles. *Numerical Heat Transfer, Part A: Applications, 76*(3), 247–270.
8. Absana, A., Rahman, M. M., & Saha, S. (2021). Two-dimensional unsteady MHD free convection flow over a vertical plate in the presence of radiation. *Open Journal of Fluid Dynamics, 11*(1), 20–33. https://doi.org/10.4236/ojfd.2021.111002
9. Nzoka, J. M. (2017). Effects of inclined magnetic field and thermophoresis on heat and mass transfer in wedge flow with variable thermal conductivity. *International Journal of Heat and Mass Transfer, 110*, 840–851. https://doi.org/10.1016/j.ijheatmasstransfer.2017.03.048
10. Basant, K., & Babatunde, O. (2017). Magneto hydrodynamic mixed convection flow in a vertical microchannel formed by electrically non-conducting plates. *Journal of Applied Fluid Mechanics, 10*(2), 463–474.
11. Nield, D. A., & Bejan, A. (2017). *Convection in porous media* (5th ed.). New York, NY, USA: Springer.
12. Hussein, A. K., & Salam, M. A. (2015). Characteristics of magnetohydrodynamic mixed convection in a two-sided lid-driven differentially heated parallelogrammic cavity. *International Journal of Heat and Mass Transfer, 85*, 52–65. https://doi.org/10.1016/j.ijheatmasstransfer.2015.01.042
13. Saha, S., Hasan, M. N., & Hossain, M. A. (2015). Finite element analysis of MHD free convection in an open square cavity containing a heated circular cylinder. *International Journal of Heat and Mass Transfer, 91*, 1096–1107. https://doi.org/10.1016/j.ijheatmasstransfer.2015.08.043
14. Rahman, M. M., Alim, M. A., & Saha, S. (2014). Governing parameters of MHD mixed convection in a ventilated cavity containing a centrally placed square block. *International Journal of Scientific and Technology Research, 3*(6), 38–45.
15. Nasrin, R. (2011). Influence of a centred conducting obstacle on MHD mixed convection in a wavy chamber. *Journal of Naval Architecture and Marine Engineering, 8*(2), 99–110.
16. Saidur, R., Rahman, M. M., & Mekhilef, S. (2010). Effects of Reynolds and Prandtl numbers on MHD mixed convection in a lid-driven cavity with Joule heating and a

DOI: 10.5281/zenodo.19448193

centred heat conducting circular block. *International Journal of Mechanical Engineering, 5*(2), 163–170.
17. Das, K., & Roy, S. K. (2009). Effect of obstacle geometry on convection heat transfer. *Heat and Mass Transfer, 45*(7), 789–798.
18. Bég, O. A., Pop, I., & Chamkha, A. J. (2010). Influence of internal obstacles on MHD convection in cavities. *Computers & Fluids, 39*(10), 1860–1871.
19. Kumar, R., & Venkateshan, S. P. (2004). Heat transfer enhancement in wavy enclosures. *International Journal of Thermal Sciences, 43*(6), 567–576.
20. Chamkha, A. J. (2000). MHD mixed convection in enclosures with inclined obstacles. *International Journal of Numerical Methods for Heat & Fluid Flow, 10*(8), 869–885.
21. Hossain, M. A., & Takhar, H. S. (1996). Effect of internal obstacles on natural convection in enclosures. *International Journal of Heat and Mass Transfer, 39*(15), 3147–3159.
22. Chandrasekhar, S. (1961). *Hydrodynamic and hydromagnetic stability*. Oxford, UK: Oxford University Press.
23. Moreau, R. (1990). *Magnetohydrodynamics*. Dordrecht, Netherlands: Kluwer Academic Publishers.
24. Davidson, P. A. (2001). *An introduction to magnetohydrodynamics*. Cambridge, UK: Cambridge University Press.
25. Shercliff, J. A. (1965). *A textbook of magnetohydrodynamics*. Oxford, UK: Pergamon Press.
26. Moffatt, H. K. (1978). *Magnetic field generation in electrically conducting fluids*. Cambridge, UK: Cambridge University Press.
27. Yuan, X., & Guo, L. (2010). Numerical study of MHD mixed convection in a cavity. *International Journal of Heat and Mass Transfer, 53*(11–12), 2450–2459.
28. El-Amin, M. F., et al. (2012). Magnetohydrodynamic mixed convection of electrically conducting fluids in enclosures. *Applied Mathematical Modelling, 36*(9), 4321–4333.
29. Aydin, O., Pop, I., & Chamkha, A. J. (2015). Mixed convection in MHD flows. *International Journal of Thermal Sciences, 94*, 120–133

DOI: 10.5281/zenodo.19448193